Influence of Cathodic Arc Current on Structure, Mechanical and Tribological Properties of TiC/a-C:H Nano-multilayer Coatings

Can Xin Tian[1], Chang Wei Zou[1,*], Ze Song Wang[1], Bing Yang[2], De Jun Fu[2], Vasuliy Olegovich Pelenovich[3] and Alexander Tolstogouzov[4]

[1]School of Physics Science & Technology, Lingnan Normal University, Zhanjiang 524048, China.
[2]School of Power & Mechanical Engineering, Wuhan University, 430072 Wuhan, China.
[3]Institute of Ion-Plasma and Laser Technologies, Academy of Sciences of Uzbekistan, 700135 Tashkent, Uzbekistan.
[4]Ryazan State Radio Engineering University, Gagarin Str. 59/1, Ryazan, 390005, Russian Federation.

(*) Correspondence: qingyihaiyanas@163.com

Abstract

A cathodic arc ion plating system was used to produce TiC/a-C:H nano-multilayer coatings on silicon and cemented carbide substrates at cathodic arc currents in the range of 30-70 A. The microstructure, surface morphology and compositions of the TiC/a-C:H nano-multilayer coatings were analyzed by transmission electron microscopy, scanning electron microscopy, Raman spectroscopy and X-ray photoelectron spectroscopy. The influence of the arc current on mechanical and tribological properties of the TiC/a-C:H nano-multilayer coatings was systemically investigated. The measurements show that the TiC/a-C:H multilayer coatings are composed of alternating layers of nanocrystalline TiC and amorphous hydrogenated carbon. The surface morphology of the TiC/a-C:H nano-multilayer coatings is controllable by the arc current. The ratio of Raman peak intensities I_D/I_G decreases and the full width at half maximum of G peaks ($FWHM_G$) increases with the increasing of arc current. The content of hydrogen decreases from 26.5 at.% to 13.7 at.% while the content of TiC increases from 0.15at. % to 2.35 at.% as the arc current increases from 30 A to 70 A. The hardness of the TiC/a-C:H nano-multilayer coatings increases continuously up to 29.5 GPa at 70 A arc current. The average friction coefficients of the coatings keep at relatively lower values in the range of 0.1-0.2 as measured against Si_3N_4 balls. The results show significant influences of the cathodic arc current on the microstructure and properties of the TiC/a-C:H nano-multilayer coatings.

Keywords: *TiC/a-C:H, Nano-multilayer coatings, Microstructure, Mechanical properties, Cathodic arc ion plating.*

1. INRODUCTION

Diamond-like carbon (DLC) coatings has attracted attention in recent decades for broad industrial applications [1-3]. DLC coatings is the general name of amorphous carbon films, including hydrogen-free amorphous carbon (a-C) and hydrogenated amorphous carbon (a-C:H) [2, 4]. Because of their high hardness, low friction coefficient, high wear resistance, chemical inertness and biocompatibility, hydrogenated amorphous carbon (a-C:H) films have been increasingly used in the automotive, tool, die, and mold industries [5-9]. Compared to the a-C films, a lower friction coefficient and a reduced abrasive wear for the a-C: H films can be achieved in drag tests [4, 10-11].

The a-C:H coatings are produced by a number of techniques including unbalanced magnetron sputtering, plasma enhanced chemical-vapor deposition (PECVD), plasma-based ion implantation and deposition (PBII&D) and high power impulse magnetron sputtering (HiPIMS). It can be seen that the hardness of the a-C:H films fabricated by unbalanced magnetron sputtering reached about 14 GPa while the friction coefficient was lower 0.1 under different CH_4/Ar ratios and bias voltage [11, 12]. The hardness and elastic modulus of a-C:H films deposited by RF glow discharge PECVD at 500 W RF power is 10 GPa and 136 MPa, respectively, and the I_D/I_G ratio is 0.66 [13]. For the a-C:H coatings deposited by high frequency unipolar pulse PECVD, when the bias voltage increases from -800 V to -1600 V, the corresponding hardness of a-C:H coatings decreases from 14.72 GPa to 12.89 GPa, the elastic recovery increases from 82.2% to 88.1%, and the tribological properties is also improved; the excellent mechanical properties are attributed to the formation of more graphitic microstructures in the amorphous carbon matrix [14]. A highest hardness of a-C:H films deposited by ion source assisted PECVD was measured to be 19±1.9 GPa [15]. With the increasing of Ar flow ratio, the hardness of the a-C:H films deposited by PBII&D increased from 13 GPa to 16 GPa while the internal stress increased from 1.25 GPa to 2.4 GPa [7]. These results indicate that the composition, microstructure and properties of the a-C:H films are strongly dependent on the deposition process. Therefore, the mechanical and tribological properties of a-C:H films can be tuned efficiently by adjusting the process parameters.

The deposited a-C:H films in the methods such as PECVD and magnetron sputtering generally have lower hardness (<20 GPa) [12-14], high stress (several GPa to 10 GPa) [16, 17], which causes poor adhesion to the substrate, and leads to peeling-off of the film from the substrate during application. In order to further improve the adhesion and the mechanical and tribological properties, various process strategies have been proposed such as doping with metallic elements or metallic carbides (Ti, Cr, Si, Ag, Cu, CrC, etc.) [9, 18-22], using metallic and grade interlayers [16, 22-24], or applying stress engineering of gradient multilayers [25]. Through the combination of Ti-doping and Ti functional gradient layer, the intrinsic stress of a-C:H could be released due to the change of the sp^3 bond content [18] or to the thermal expansion coefficients mismatch [16]. The higher hardness, stronger adhesion, lower friction coefficient and better wear resistance can be fabricated by utilization of Cr interlayers [23]. The residual stress of 8 μm thick a-C:H coatings is between 0.42 GPa and 0.84 GPa and a maximum critical load of 74 N and a hardness of over 26 GPa are fabricated through the use of the Cr/CrCx/CrC gradient multilayer structure [25].

Cathodic arc ion plating with a high ionization rate of 70-90% can also be used for preparation of a-C:H films doped with Cr, Mo and W [26-29]. The Cr-, Mo- and W-doped a-C:H coatings deposited by arc ion plating have low ratios of sp^2/sp^3, and their hardness is much higher (25 GPa) while the friction coefficient is lower (~0.2). Incorporation of metals into a-C:H films forms a nano-composite or nano-multilayer structure with improved physical properties. In this study, a-C:H coatings with high ratios of sp^2/sp^3 were deposited under various arc currents by cathode arc ion plating. A titanium interlayer was used to optimize the adhesion of a-C:H coatings and a nano-multilayer structure with TiC layers was used to improve the microstructure, mechanical and tribological properties of the TiC/a-C:H nano-multilayer coatings.

2. EXPERIMENT DETAILS

The nano-multilayer TiC/a-C:H coatings were deposited by using a hollow arc ion

source assisted cathodic arc ion plating system in argon and C_2H_2 atmosphere. Metal Ti targets were used as the solid sources. The Ti cathode and hollow arc ion sources are symmetrically arranged on the walls of the vacuum chamber. Silicon and cemented carbide were used as substrates. The Si substrates were coated for the measurements of scanning electronic microscopy (SEM), Raman micro-spectrometer (Raman), X-ray photo-electron spectroscopy (XPS), and for preparation of transmission electron microscopy (TEM) samples, while the cemented carbide substrates were used for evaluation of mechanical properties. The chamber was first evacuated to less than 5×10^{-3} Pa and heated up to 300°C. Prior to film deposition, Ar^+ etching procedures at a bias voltage of 800 V and a chamber pressure of 2 Pa were carried out to clean the surface of the substrates. Subsequently Ti ion bombardment was carried out to further remove any contamination on the substrate surfaces with -800 V bias at 0.02 Pa Ar pressure. The first Ti interlayers were deposited by sputtering of the Ti targets at a bias voltage of 100 V, an arc current of 70 A, and an Ar pressure of 0.5 Pa for 5 min. Then the C_2H_2 gas was fed up into the chamber through the hollow arc ion source to deposit TiC/a-C:H nano-multilayer coatings for 30 min. The flow rates of Ar and C_2H_2 gases were fixed at 100 sccm and 200 sccm, respectively. The thickness of TiC/C:H was about 1.8 μm. The details of the deposition parameters are listed in Table 1.

The microstructure of the coatings was observed by transmission electron microscopy (TEM, JEOL JEM 2010). The surface morphologies and thickness of the coatings were measured by scanning electronic microscopy (SEM, FEI Sirion IMP SEM). The Raman spectra of the coatings were recorded by using a laser confocal Raman micro-spectrometer (Lab RAM HR 800 UV) operated with a 514.5 nm ion laser. The hydrogen content of the TiC/a-C:H coatings was estimated from the photoluminescence background in the Raman spectra of the films [6, 8]. The chemical bonding states were investigated by X-ray photoelectron spectroscopy by using Mg Ka (1253.6 eV) X-ray radiation on Kratos 2AXIS2HS XPS system.
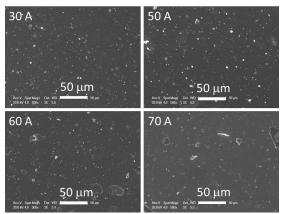
Table 1. *Deposition parameters of TiC/a-C:H nano-multilayer coatings.*

Parameters	Values
Target material (Ti)	*99.6%*
Bias voltage (V)	*Etching: -800, deposition: -100*
Cleaning and reactive gases	*Ar and C_2H_2*
Working pressure (Pa)	*Etching: 0.02, deposition: 0.5*
Substrate temperature (°C)	*300*
Rotation speed (rpm)	*1*
Target current (A)	*30, 50, 60, 70*

The hardness of TiC/a-C:H nano-multilayer coatings was measured by a nanoindenter (Agilent Nano Indenter G200) at a load of 30 mN and taking the average of 6 random values. The wear behavior was evaluated through sliding tests using a conventional ball-on-disc wear apparatus (MS-T3000), with Si_3N_4 balls (3 mm in diameter) being used as counterpart materials. The sliding tests were conducted with a sliding speed of 0.02 m/s under a load of 5 N at ambient air with a temperature of around 30°C and a relative humidity of 70-75%. The sliding time lasted for 30 min and the friction coefficients were recorded during the test.
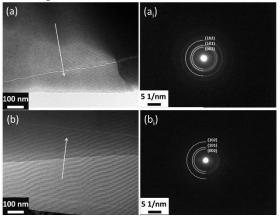
3. RESULTS AND DISCUSSION

Fig. 1 shows the surface morphologies of the TiC/a-C:H nano-multilayer coatings under different cathodic arc currents. It can be seen that when the arc current is lower than 50 A, the number of macroparticles is

increased with increasing arc current. This can be attributed to the heating effect under the arc current. However, when the arc current increases up to 70 A, the number of macroparticles is reduced while some debris and shallow pits are observed. The reduction of the macroparticle number can be attributed to target poisoning, namely, when the target current exceeds a certain value, it promotes the formation of high-melting-point TiC layers covering parts of the target surface. The debris and shallow pits may come from the higher internal stress of the a-C:H coatings deposited at higher target arc currents. It is well known that the internal stress of the a-C coatings with more sp^3 bonds is higher [30]. As shown in Figs. 4 and 5, more sp^3 carbon atoms are detected in TiC/a-C:H with the increase of arc current.
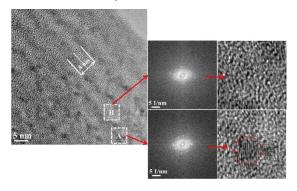

Figure 1. Surface morphologies of the TiC/a-C:H nano-multilayer coatings deposited at various arc currents.

Figs. 2 (a)-(b) show the cross-sectional TEM bright field images of TiC/a-C:H nano-multilayer coatings deposited on Si substrates at 30 A and 50 A. It can be seen that the TiC/a-C:H coatings exhibits a nano-multilayered structure. The gray areas are the TiC layers, and white areas are a-C:H. The interfaces between TiC and a-C:H layers are relatively fuzzy. The modulation period of the TiC/a-C:H coatings is about 6~10 nm. Figs. 2 (a_i) and (b_i) show the corresponding selected area electron diffraction (SAED) of TiC/a-C:H nano-multilayer coatings. The SAED

patterns are typical polycrystalline diffraction rings, corresponding to TiC (002), (101) and (102) orientations, and we can conclude that the coating is a polycrystalline structure. To investigate more details of TiC/a-C:H nano-multilayer coatings, high resolution transmission electron microscopy (HRTEM) was measured and shown in Fig. 3. The right is the corresponding fast Fourier transformation patterns and the inverse fast Fourier transform images of the white square area A (TiC layer) and B (a-C:H layer), respectively. It is clearly seen that there exist TiC nanocrystallites and the grain size is about 3-5 nm in area A. The nano-multilayered structure of TiC/a-C:H coating is composed of alternating layers of nano-crystallite TiC and hydrogenated amorphous carbon. In the Fig. 2 (a), the white line of bright-field image may be caused by sample's cracking.
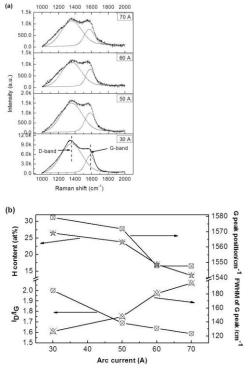

Figure 2. Cross-sectional TEM bright-field image of TiC/a-C:H nano-multilayer coatings deposited at arc currents of 30 A (a) and 50 A (b) and the corresponding diffraction patterns (ai) and (bi). The arrows indicate growth direction.

Figure 3. High-resolution cross-sectional TEM image of TiC/a-C:H nano-multilayer coatings deposited at 50 A arc current and the corresponding fast Fourier transformed patterns and inverse fast Fourier transform image of the selected areas A (nanocrystallite TiC layer) and B (amorphous C:H layer).

Fig. 4 (a) shows the Raman spectra of the TiC/a-C:H nano-multilayer coatings deposited at different arc currents. The Raman spectra acquired from different samples can be fitted into two Gaussian peaks: D and G peaks, which are around 1355 cm^{-1} and 1580 cm^{-1}, respectively [31]. The peak G is due to the bond stretching of all pairs of sp^2 atoms in both rings and chains. The peak D is due to the breathing modes of sp^2 atoms in rings [32-33]. It should be noticed that the intensity of the D peak of the coatings decreases gradually with the increase of the arc current. The changes of intensity ratio of D peak and G peak (I_D/I_G), as well as the G-peak position and its $FWHM_G$ are shown in Fig. 4 (b), reflecting the carbon lattice structure. Here I_D/I_G is the ratio of the peak heights. With increasing of the arc current, the ratio of I_D/I_G decreases from 2 to 1.59 and G-peak position shifts from 1580 cm^{-1} to 1547 cm^{-1}. It is seen that there is an obvious downshift of the G-peak position when the deposition arc current is increased from lower (30A, 50A) to higher (60A, 70A) values, while there is no significant change in the G-peak position for the coatings deposited under the high arc currents (60, 70A). It is empirically known that the I_D/I_G decreases and G peak position shifts downwards with the decrease of graphitic component in the coatings. This suggests the decrease in the size and number of clustering of sp^2 phase [13, 34-36]. The $FWHM_G$ is related to the structure disorder in the carbon bonding of the a-C films [37-38]. Therefore, as a result of the high deposition arc current, the $FWHM_G$ is high, causing disordered sp^2 clusters in the TiC/a-C:H nano-

multilayer coatings. The hydrogen content of the TiC/a-C:H nanomultilayer coatings is provided in Fig. 4 (b). It reveals that when the arc current increases from 30 A to 70 A, the content of hydrogen apparently decreases from 26.5 at.% to 13.7 at.%.
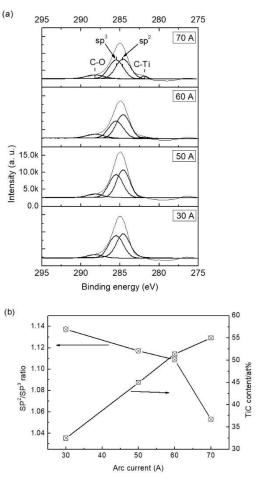

Figure 4. Raman spectra (a), ID/IG ratio, H content, G-peak position and the FWHMG (b) of TiC/a-C:H nano-multilayer coatings deposited at various arc currents.

XPS analysis gives extensive information about the chemical composition and bonding states of the coatings. Fig. 5 (a) shows core level spectra of C1s electrons of the TiC/a-C:H nano-multilayer coatings deposited on Si substrates at different arc currents. The XPS spectra were fitted by using the XPSPEAK software. The typical C1s peak is fitted into four components around 281.7 eV, 284.6 eV, 285.5 eV, and 288.2 eV, which correspond to C-Ti, sp^2 carbon bonds, sp^3 carbon bonds, and $C-O_x$, respectively [39]. By increasing the arc current, compared with the fitting sp^2 peaks, the relative intensities of the fitting sp^3 peaks are higher. The increased

intensity of fitting sp^3 peaks is believed to result from the increasing sp^3 content. The plasma energy is the main parameter to influence the content of sp^3 bonding in pure amorphous carbon films [40-41], and the formation energy for the sp^3 hybrid orbit is higher than that of the sp^2 hybrid orbit [42]. Therefore, with the increase of the deposition arc current, more Ti ions with proper energy were incorporate to the coatings during deposition, which promoted the formation of sp^3 bonds. There is no obvious peak of C-Ti bonds located at 281.7 eV for coatings deposited with low arc currents (30 A and 50 A), which is believed that the TiC content is low under these conditions or influenced by the surface amorphous carbon layer. As seen from Fig. 5 (b), the contents of the TiC phase increases from 0.15% to 2.35 at% as the arc current increases from 30 A to 70 A. The contents of TiC in the surface of the as-deposited TiC/a-C:H coatings are calculated from fitting C1s spectra. According to other studies [43], the evolution of chemical state for Ti is related to the Ti target current, which means the increase of the Ti content. When the Ti target current is lower, Ti ions from Ti targets cannot bond with C ions due to their low energy and quantity. Only when the energy and quantity of Ti ions increase to the threshold with increasing Ti target current, the Ti ions can bond with C and form TiC [44]. The ratio of the sp^2/sp^3 within the as-deposited TiC/a-C:H films can be calculated approximately from the fitting C1s shown in Fig. 5 (b). The results show that the sp^2/sp^3 ratio decreases from 1.14 to 1.05 with the arc current increasing from 30 A to 70 A. As shown in Ref. [45], the sp^2 content of a-C films deposited by magnetron sputtering increases with increasing Ti target current, but in this study the TiC/a-C:H coatings shows the opposite tendency. This may be due to the different energy of Ti ions in the process of arc ion plating.
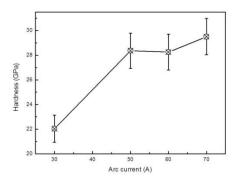
Fig. 6 shows the relationship between the hardness of the TiC/a-C:H nano-multilayer

coatings deposited on cemented carbide substrates.

Figure 5. *(a) XPS spectra of C1s core levels of the TiC/a-C:H nano-multilayer coatings deposited at various arc currents, (b) sp2/sp3 ratio and contents of TiC phase at the surface of the TiC/a-C:H coatings from fitting C 1s spectra.*
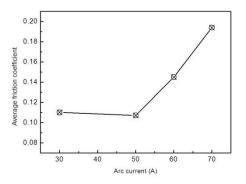
The hardness increases from 22 GPa to 29.5 GPa when the arc current increases from 30 A to 70 A. This clearly shows that the arc current has a remarkable effect on the hardness of the TiC/a-C:H nano-multilayer coatings. The hardness of the TiC/a-C:H nano-multilayer coatings deposited at 30 A is obviously lower than that of the coatings deposited at 50-70 A. It is noted that the minimum hardness value 22 GPa of the TiC/a-C:H nano-multilayer coatings is higher than that of some a-C and a-C:H films as reported in literature [46]. The higher hardness of the TiC/a-C:H nano-multilayer coatings is attributed to the microstructure of nano-multilayer, as

verified by TEM analysis (as shown in Figs. 2 and 3). The variation the hardness of the TiC/a-C:H nano-multilayer coatings is attributed to the variation of the microstructure with increasing arc current. The increased arc current can provide sufficient Ti to react with C to form the hard TiC phase, leading to the improvement of hardness [44]. As shown in Fig. 5 (b), with the increase of arc current, the content of the TiC phase in the coatings of TiC/a-C:H increase, and the hardness of the TiC/a-C:H coatings is improved. One reason for the improved hardness in this case is the increased content of sp^3 in the TiC/a-C:H nano-multilayer coatings with increasing arc current (as shown in Figs. 4 and 5). According to Ref. [6, 47], if the G-peak position is in the high-wavenumber region above 1540 cm^{-1}, then the films have the characteristics of graphite-like carbon, and the hardness increases with increasing $FWHM_G$ of the a-C:H coatings. The $FWHM_G$ depends on the number of C-C sp^3 bonds and can be used to evaluate the mechanical properties of the films [48].

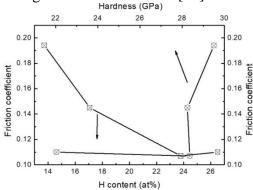**Figure 6.** *Hardness of TiC/a-C:H nano-multilayer coatings deposited at various arc currents.*

Fig. 7 shows the average friction coefficient of TiC/a-C:H nano-multilayer coatings deposited on cemented carbide substrates as a function of arc current. It is found that the friction coefficient of the nano-multilayer coatings increases from 0.11 to 0.19 when the arc current increase from 30 A to 70 A. The friction coefficient of the nano-multilayer coatings keeps at a relative low value about 0.1 when the arc current is low (30 A and 50 A). The variation of the average friction coefficient is believed to relate with the nano-multilayer structure of TiC/a-C:H with different sp^2 and sp^3 contents. The coatings possessing a greater sp^2 content provide more effective solid lubrication and minimizing both wear and friction [49]. As shown in Fig. 5 (b), as the arc current increases, the ratio of sp^2/sp^3 decreases, which means the coatings contains less sp^2 C-C. At the lower content of sp^2, the friction coefficient of a-C:H films is inevitably higher.

Figure 7. *Average friction coefficients of TiC/a-C:H nano-multilayer coatings deposited at various arc currents.*

The correlations between the H content and hardness of TiC/ a-C:H coatings and their friction coefficients are shown in Fig. 8. It is observed that the friction coefficient of TiC/a-C:H coatings decreases with the increasing of hydrogen content, and increases with the increase of hardness. Researchers found that hydrogen can passivate the dangling bonds generated on the friction interfaces during sliding [50-51]. Such hydrogen passivation prevents the chemical reaction of highly active dangling bonds, resulting in friction reduction. In Refs. [8, 52] investigation on the relationship between friction coefficients of a-C:H films and H content have shown that the friction coefficients decrease with increasing hydrogen content. The content of sp^3 bonds in the a-C:H film is responsible for the high hardness, and the higher hardness is accompanied with

higher shear strength and higher friction coefficients [8]. It is worth noting that the TiC/a-C:H coatings with lower friction coefficients has relationship with other factors such as high humidity during the sliding test. Marino et al. reported the formation of four water monolayers in 75% relative humidity on the surface of hydrogenated a-C:H films [53]. This water layer acts as a boundary lubricant, resulting in a reduced friction [54].

Figure 8. *Correlation between the H content and hardness of TiC/a-C:H coatings and their friction coefficients.*

4. CONCLUSION

The TiC/a-C:H coatings deposited by using a cathodic arc system in C_2H_2 and Ar ambient under different arc currents showed an alternating structure of nano-multilayers of TiC and a-C:H. The arc current has evident influence on the microstructure, the mechanical and friction properties of the TiC/a-C:H nano-multilayer coatings. The Raman scattering analysis showed that with increasing arc current, the I_D/I_G ratio decreases and the G-peak position downshifts while the FWHM$_G$ is enhanced. The content of hydrogen decreases from 26.5 at. % to 13.7 at. % while the contents of TiC increase from 0.15 at.% to 2.35 at.% as the arc current increases from 30 A to 70 A. The hardness increases with increasing arc current and a highest hardness of 29.5 GPa was achieved at a 70 A arc current. Furthermore, the average friction coefficients of the coatings increase from 0.11 to 0.19 with the increase of the arc current. In summary, the mechanical and friction performance of TiC/a-C:H coatings can be enhanced significantly by building the nano-multilayer structure. The higher hardness of TiC/a-C:H nano-multilayer coatings should be attributed to the alternating structure of the nano-multilayers while the lower friction coefficient is influenced by content of sp^2 and sp^3. The cathodic arc current has controlling influence on the structure and properties of the TiC/a-C:H nano-multilayer coatings.

REFERENCES

1. Ye, Y. W., Wang, Y. X., Ma, X. L., Zhang, D. Z., Wang, L. P., Li, X. G., "Tribocorrosion behaviors of multilayer PVD DLC coated 304L stainless steel in seawater", *Diamond & Related Materials*, 79 (2017) 70-78.
2. Eurídice, W. A., Leite, N. B., Gelamo, R. V., Buranello, P. A., Silva, M. V., Oliveira, C. J., Lopez, R. F., Lemos, C. N., Siervo, A., Moreto, J. A., "a-C:H films produced by PECVD technique onto substrate of Ti6Al4V alloy: Chemical and biological responses", *Applied Surface Science*, 503 (2020) 144084.
3. Ye, Y. W., Wang, C. H., Wang, Y. X., Liu, W., Liu, Z. Y., Li, X. G., "The influence of different metallic counterparts on the tribological performance of nc-CrC/GLC in seawater", *Surface & Coatings Technology*, 325 (2017) 689-696.
4. Tillmann, W., Ulitzka, H. N., Lopes Dias, F., Stangier, D., Thomann, C. A., Moldenhauer, H., Debus, J., "Effects of acetylene flow rate and bias voltage on the structural and tribomechanical properties of sputtered a-C:H films", *Thin Solid Films,* 693 (2020) 137691.

5. Wang, C. T., Ye, Y. W., Guan, X. Y., Hu, J. M., Wang, Y. X., Li, J. L., "An analysis of tribological performance on Cr/GLC film coupling with Si3N4, SiC, WC, Al2O3 and ZrO2 in seawater", *Tribology International*, 96 (2016) 77-86.

6. Choi, J., Hatta, T., "Structural changes of hydrogenated amorphous carbon films deposited on steel rods", *Applied Surface Science*, 357 (2015) 814-818.

7. Hirata, Y., Onishi, K. Choi, J., "Effect of Ar+ ion assist on the properties of a-C:H films deposited on a trench", *Thin Solid Films,* 631 (2017) 57–63.

8. Ishikawa, T., Choi, J., "The effect of microstructure on the tribological properties of a-C:H films", *Diamond & Related Materials*, 89 (2018) 94-100.

9. Thukkaram, M., Vaidulych, M., Kylian, O., Hanus, J., Rigole, P., Aliakbarshirazi, S., Asadian, M., Nikiforov, A., Tongel, A. V., Biederman, H. Coenye, T., Laing, G. D., Morent, R., Wilde, L. D., Verbeken, K., Geyter, N. D. "Investigation of Ag/a-C:H nanocomposite coatings on titanium for orthopedic applications", *ACS Applied Materials & Interfaces*, 12 (2020) 23655-23666.

10. Marchon, B., Vo, P. N., Khan, M. R., "Structure and mechanical properties of hydrogenated carbon films prepared by magnetron sputtering", *IEEE transactions on magnetics*, 27 (1991) 5160-5162.

11. Wang, Y. X., Ye, Y. P., Li, H. X., Ji, L., Chen, J. M., Zhou, H. D., "A magnetron sputtering technique to prepare a-C:H films: Effect of substrate bias", *Applied Surface Science*, 257 (2011) 1990-1995.

12. Wang, Y. X., Ye, Y. P., Li, H. X., Zhang, G. A., Wang, S. C., Wood, R. J. K., Xue, Q. J., "Microstructure and tribological properties of the a-C:H films deposited by magnetron sputtering with CH$_4$/Ar mixture", *Surface & Coatings Technology*, 205 (2011) 4577–4581.

13. Gou, W., Li, G. Q., Chu, X. P., Zhong, B., "Effect of negative self-bias voltage on microstructure and properties of DLC films deposited by RF glow discharge", *Surface & Coatings Technology*, 201 (2007) 5043–5045.

14. Wang, J., Cao, Z. Y., Pan, F. P., Wang, F. G., Liang, A. M., "Tuning of the microstructure, mechanical and tribological properties of a-C:H films by bias voltage of high frequency unipolar pulse", *Applied Surface Science*, 356 (2015) 695–700.

15. Zolkin, A., Semerikova, A., Chepkasov, S. Khomyakov M., "Investigation of the properties of hydrogenated carbon films (a-C:H) deposited on germanium using a linear anode layer ion source", *Materials Today, Proceedings*, 4 (2017) 11500-11504.

16. Wang, P., Wang, X., Xu, T., Liu, W. M., Zhang, J. Y., "Comparing internal stress in diamond-like carbon films with different structure", *Thin Solid Films*, 515 (2007) 6899-6903.

17. Ban, M., Hasegawa, T., Fujii, S., Fujioka, J., "Stress and structural properties of diamond-like carbon films deposited by electron beam excited plasma CVD", *Diamond and Related Materials*, 12 (2003) 47-56.

18. Zhou, Y. F., Li, L. L., Shao, W., Chen, Z. H., Wang, S. F., Xing, X. L., Yang, Q. X., "Mechanical and tribological behaviors of Ti-DLC films deposited on 304 stainless steel: Exploration with Ti doping from micro to macro", *Diamond & Related Materials*, 107 (2020) 107870.

19. Chang, Y. Y., Wang, D. Y., "Structural and electrical properties of Cr doped a-C:H films synthesized by a cathodic-arc activated deposition process", *Surface & Coatings Technology*, 200 (2006)3170-3174.

20. Wang, K., Yang, B. P., Zhang, B., Bai, C. N., Mou, Z. X., Gao, K. X., Yushkov, G., Oks, E., "Modification of a-C:H films via nitrogen and silicon doping: The way to the super lubricity in moisture atmosphere", *Diamond & Related Materials*, 107 (2020) 107873.

21. Nißen, S., Heeg, J., Wienecke, M., Behrend, D., Warkentin, M., Rokosz, K., Gaiaschi, S., Chapon, P., "Surface Characterization and Copper Release of a-C:H:Cu Coatings for Medical Applications", *Coatings*, 9 (2020) 119.

22. Tillmann, W., Dias, N. F. L., Stangier, D., Maus-Friedrichs, W., Gustus, R., Thomann, C. A., Moldenhauer, H., Debus, J., "Improved adhesion of a-C and a-C:H films with a CrC interlayer on 16MnCr5 by HiPIMS-pretreatment", *Surface & Coatings Technology*, 375 (2019) 877-887.

23. F. Shahsavari, M. Ehteshamzadeh, M. Hassan Amin, Barlow, A. J., "A comparative study of surface morphology, mechanical and tribological properties of DLC films deposited on Cr and Ni nanolayers", *Ceramics International*, 46 (2020) 5077-5085.

24. Wei, C. H., Yang, J. F., Tai, F. C., "The stress reduction effect by interlayer deposition or film thickness for diamond like carbon on rough surface", *Diamond & Related Materials*, 19 (2010) 518-524.

25. Liu, L. L., An, X. K., Ma, Z. Y., Wu, Z. Z., Tang, W., Lin, H., Fu, R. K. Y., Tian, X. B., Chu, P. K., Pan, F., "Hard and adherent a-C:H gradient coatings by stress engineering", *Journal of Alloys and Compounds*, 765 (2018) 921-926.

26. Jiang, K. M., Zhao, D. Q., Jiang, X., Huang, Q., Miao, L. J., Lu, H. M., Li, Y., "Electronic-structure, corrosion and mechanical properties of nc-CrC/aC:H films deposited by multi-arc ion plating", *Journal of Alloys and Compounds*, 750 (2018) 560-569.

27. Wang, D. Y., Weng, K. W., Chang, C. L., Guo, X. J., "Tribological performance of metal doped diamond-like carbon films deposited by cathodic arc evaporation", *Diamond and Related Materials*, 9 (2000) 831-837.

28. Wang, W., Pelenovich, V. O., Yousaf, M. I., Yan, S. J., Han, B., Wang, Z. S., Tolstogouzov, A. B., Kumar, P., Yang, B., Fu, D. J., "Microstructure, mechanical and tribological properties of WC/a-C:H coatings deposited by cathodic arc ion-plating", *Vacuum*, 132 (2016) 31-39.

29. Wang, L. L., Wang, R.Y., Yan, S. J., Zhang, R., Yang, B., Zhang, Z. D., Huang, Z. H., Fu, D. J., "Structure and properties of Mo-containing diamond-like carbon films produced by ion source assisted cathodic arc ion-plating", *Applied Surface Science*, 286 (2013) 109-114.

30. Mabuchi, Y., Higuchi, T., Weihnacht, V., "Effect of sp^2/sp^3 bonding ratio and nitrogen content on friction properties of hydrogen-free DLC coatings", *Tribology International*, 62 (2013) 130-140.

31. Wang, Y. F., Gao, K. X., Zhang, B., Wang, Q., Zhang, J. Y., "Structure effects of sp2-rich carbon films under super-low friction contact", *Carbon*, 137 (2018) 49-56.

32. Zhang, X. Q., Ke, P. L., Wang, A. Y., Huang, M. D., Kim, K. H., "Effect of substrate bias on microstructure and tribological performance of GLC films using hybrid HIPIMS technique", *Trans. Nonferrous Met. Soc. China*, 22 (2012) s740-s744.

33. Zhang, J. W., Zhou, S. G., Wang, Y. X., Wang, Y. C., Wang, C. T., Lu, X., Mao, C. L., Chen, S. J., Lu, X. J., Wang, L. P., "Enhancing anti-corrosion and antifouling properties of Cu/GLC composite film for marine application", *Surface & Coatings Technology*, 375 (2019) 414-426.

34. Alawajji, R. A., Kannarpady, G. K., Nima, Z. A., Kelly, N., Watanabe, F., Biris, A. S., "Electrical properties of multilayer (DLC-TiC) films produced by pulsed laser deposition", *Applied Surface Science*, 437 (2018) 429-440.

35. Ferrari, A. C., Robertson, J., "Interpretation of Raman spectra of disordered and amorphous carbon", *Physical review B*, 61 (2000) 14095.

36. Capote, G., Corat, E, J., Trava-Airoldi, V. J., "Deposition of amorphous hydrogenated carbon films on steel surfaces through the enhanced asymmetrical modified bipolar pulsed-DC PECVD method", *Surface & Coatings Technology*, 260 (2014) 133-138.

37. Dong, D., Jiang, B. L., Li, H. T., Du, Y. Z., Yang, C., "Effect of graphite target power density on tribological properties of graphite-like carbon films", *Applied Surface Science*, 439 (2018) 900-909.

38. Khatir, S., Hirose, A., Xiao, C., "Coating diamond-like carbon films on polymer substrates by inductively coupled plasma assisted sputtering", *Surface & Coatings Technology*, 253 (2014) 96-99.

39. Cai, Y., Wang, R.Y., Liu, H. D., Luo, C., Wan, Q., Liu, Y., Chen, H., Chen, Y. M., Mei, Q. S., Yang, B., "Investigation of (Ti:N)-DLC coatings prepared by ion source assisted cathodic arc ion-plating with varying Ti target currents", *Diamond & Related Materials*, 69 (2016) 183-190.

40. Lacerda, R. G., Hammer, P. C., Lepienski, M., Alvarez, F., Marques, F. C., "Hard graphitic-like amorphous carbon films with high stress and local microscopic density", *Journal of Vacuum Science & Technology A*, 19 (2001) 971.

41. Lifshitz, Y., Lempert, G. D., Grossman, E., Avigal, I., Uzan-Saguy, C., Kalish, R., Kulik, J., Marton, D., Rabalais, J. W., "Growth mechanisms of DLC films from C+ ions: experimental studies", *Diamond and Related Materials*, 4 (1995) 318-323.

42. Wang, Z. P., Feng, L. J., Shen, W. Z., "Study on the property of low friction complex graphite-like coating containing tantalum", *Results in Physics*, 8 (2018) 41-47.

43. Jo, Y. J., Zhang, T. F., Son, M. J., Kim, K. H., "Synthesis and electrochemical properties of Ti-doped DLC films by a hybrid PVD/PECVD process", *Applied Surface Science*, 433 (2018) 1184-1191.

44. Wang, Y. X., Wang, L. P., Xue, Q. J., "Influence of Ti target current on microstructure and properties of Ti-doped graphite-like carbon films, *Trans. Nonferrous Met. Soc. China*, 22 (2012) 13721380.

45. Zhang, S., Bui, X. L., Fu, Y. Q., "Magnetron-sputtered nc-TiC/a-C(Al) tough nanocomposite coatings", *Thin Solid Films*, 467 (2004) 261-266.

46. Baptista, D. L., Zawislak, F. C., "Hard and sp^2-rich amorphous carbon structure formed by ion beam irradiation of fullerene, a-C and polymeric a-C:H films", *Diamond & Related Materials*, 13 (2004) 1791-1801.

47. Choi, J., Ishii, K., Kato, T., Kawaguchi, M., Lee, W., "Structural and mechanical properties of DLC films prepared by bipolar PBII&D", *Diamond & Related Materials*, 20 (2011) 845-848.

48. Casiraghi, C., Ferrari, A. C., Robertson, J., "Raman spectroscopy of hydrogenated amorphous carbons", *Physical Review B*, 72 (2005) 085401.

49. Fujisawa, N., Swain, M. V., James, N. L., Woodard, J. C., Tarrant, R. N., Mckenzie, D. R., "Carbon coating of Ti-6Al-4V for reduced wear in combined impact and sliding applications", *Tribology International*, 36 (2003) 873-882.

50. Erdemir, A., Eryilmaz, O. L., Nilufer, I. B., Fenske, G. R., "EVect of source gas chemistry on tribological performance of diamond-like carbon films", *Diamond and Related Materials*, 9 (2000) 632-637.

51. Erdemir, A., "The role of hydrogen in tribological properties of diamond-like carbon films", *Surface and Coatings Technology*, 146-147 (2001) 292-297.
52. Suzuki, M., Ohana, T., Tanaka, A., "Tribological properties of DLC films with different hydrogen contents in water environment", *Diamond & Related Materials*, 13 (2004) 2216-2220.
53. Marino, M. J., Hsiao, E., Bradley, L. C., Eryilmaz, O. L., Erdemir, A., Kim, S. H., "Is Ultra-Low Friction Needed to Prevent Wear of Diamond-Like Carbon (DLC) An Alcohol Vapor Lubrication Study for Stainless Steel/DLC Interface", *Tribological Letters*, 42 (2011) 285-291.
54. Xiang, D. D., Sui, X. D., Tan, X. P., Hao, J. Y., Wang, Z. W., Liao, Z. H., Liu, W. Q., Tor, S. B., "Improving biotribological properties and corrosion resistance of CoCrMo alloy via a Cr-GLC nanocomposite film in simulated body fluids", *Surface & Coatings Technology*, 378 (2019) 124840.